Published OnlineFirst August 29, 2013; DOI: 10.1158/1078-0432.CCR-13-1485

Clinical Cancer Research

Nab-Paclitaxel Is an Active Drug in Preclinical Model of Pediatric Solid Tumors

Libo Zhang[1,2], Paula Marrano[2], Sushil Kumar[4], Michael Leadley[2], Evelyn Elias[2], Paul Thorner[2,4], and Sylvain Baruchel[1,3,4]

Abstract

Purpose: To investigate the antitumor effect of nab-paclitaxel, an albumin-stabilized nanoparticle formulation of paclitaxel, on pediatric solid tumor models.

Experimental Design: A panel of three rhabdomyosarcoma, one osteosarcoma and seven neuroblastoma cell lines were exposed to increasing concentrations of nab-paclitaxel *in vitro*. Cell viability was evaluated using the Alamar Blue Assay. Antitumor effect was further assessed *in vivo* in NOD/SCID xenograft and metastatic neuroblastoma mouse models. Tumor sections were analyzed by immunohistochemistry for cleaved caspase-3 and phospho-histone H3. Plasma and intratumoral paclitaxel concentrations were measured by liquid chromatography–mass spectrometry. Ratio of intratumoral and plasma concentration was compared between nab-paclitaxel and paclitaxel treatment groups.

Results: Nab-paclitaxel displayed significant cytotoxicity against most pediatric solid tumor cell lines *in vitro* in a dose-dependent manner. *In vivo*, nab-paclitaxel showed antitumor activity in both rhabdomyosarcoma (RH4 and RD) and neuroblastoma [SK-N-BE(2) and CHLA-20] xenograft models. In the SK-N-BE (2) metastatic model, nab-paclitaxel treatment significantly extended animal survival compared with control ($P < 0.01$). Nab-paclitaxel treatment induced tumor cell-cycle arrest and apoptosis *in vivo*. In the RH4 model, increased local relapse-free intervals were observed with nab-paclitaxel treatment (37.7 ± 3.2 days) comparing with paclitaxel (13.6 ± 2.07 days). Local relapsed tumors following paclitaxel treatment proved to be paclitaxel-resistant and remained responsive to nab-paclitaxel. Mechanistically, a higher tumor/plasma paclitaxel drug ratio in favor of nab-paclitaxel was observed.

Conclusions: Nab-paclitaxel showed significant antitumor activity against all pediatric solid tumors associated with an enhanced drug intratumor delivery. Furthermore, testing of nab-paclitaxel in pediatric solid-tumor patient population is under development. *Clin Cancer Res; 19(21); 5972–83. ©2013 AACR.*

Introduction

Solid tumors make up about 60% of all pediatric cancers (1). The most common types of solid tumors in children include brain tumors, neuroblastoma, rhabdomyosarcoma, Wilms' tumor, and osteosarcoma. Although significant progress has been made during the last decades in the treatment and prognosis of pediatric malignancies, high mortality is still prevalent in patients with advanced, unresectable, or high-grade disease (2). Rhabdomyosarcoma is the most common pediatric soft-tissue sarcoma and the third most common extracranial solid tumor in children following neuroblastoma and Wilm's tumor, with an annual incidence of 4 to 7 cases per million children under the age of 16 years (3, 4). Multimodal treatment has significantly improved survival to approximately 70%. Although a majority of patients achieve a complete remission with primary therapy, a substantial number still experience recurrences with poor prognosis (5). In addition, at least 15% children with rhabdomyosarcoma present with metastatic disease The Intergroup Rhabdomyosarcoma Study Group (IRSG), and their prognosis has not improved significantly in the last 15 years (6).

Neuroblastoma is the most common extracranial childhood malignancy. It accounts for 8% to 10% of all pediatric malignancy and is responsible for 15% of all childhood cancer-related deaths (7). Despite intensive treatment protocols including megatherapy with hematopoietic stem cell transplantation and immunotherapy, the prognosis of patients with this malignancy remains poor. Disease-free survival is only about 30% for metastatic disease compared with 95% for localized tumors (8, 9).

Paclitaxel, originally isolated from *Taxus brevifolia* (Pacific yew), is a cytotoxic microtubule stabilizing agent that

Authors' Affiliations: [1]New Agent and Innovative Therapy Program; [2]Department of Paediatric Laboratory Medicine; [3]Division of Hematology and Oncology, Department of Paediatrics, The Hospital for Sick Children; and [4]Institute of Medical Sciences, University of Toronto, Toronto, Canada

Corresponding Author: Sylvain Baruchel, The Hospital for Sick Children, Room 9418, Black Wing, 555 University Avenue, Toronto, Ontario M5G 1X8, Canada. Phone: 416-813-5977/7795; Fax: 416-813-5327; E-mail: sylvain.baruchel@sickkids.ca

doi: 10.1158/1078-0432.CCR-13-1485

Published OnlineFirst August 29, 2013; DOI: 10.1158/1078-0432.CCR-13-1485

Translational Relevance

Paclitaxel has been used widely for the treatment of adult solid tumors, but it has shown minimal activity in pediatric solid tumors. Here, we evaluated a novel, solvent-free formulation of paclitaxel, nab-paclitaxel, in pediatric solid tumor models. Nab-paclitaxel is effective against both rhabdomyosarcoma and neuroblastoma in preclinical models. We also showed that nab-paclitaxel is more active than paclitaxel in all tumor models tested. Paclitaxel-relapsed tumors developed resistance against paclitaxel treatment, but those tumors remained responsive to nab-paclitaxel treatment. Mechanistically, elevated intratumor and correspondingly lower plasma paclitaxel levels were observed with nab-paclitaxel compared with paclitaxel, resulting in higher tumor/plasma paclitaxel drug ratio for nab-paclitaxel. Therefore, this preclinical study supports further testing of nab-paclitaxel in pediatric solid-tumor patient population.

stabilizes microtubules and as a result, interferes with the normal breakdown of microtubules during cell division and lead to mitotic arrest (10). This mitotic arrest triggers the mitotic spindle checkpoint and results in apoptosis (10). Paclitaxel has also been shown to mediate apoptosis through pathways that may be independent of gross microtubule dysfunction (11–13). Paclitaxel is widely used in the treatment of various malignancies, including ovarian cancer, breast cancer, non–small cell lung carcinoma (NSCLC), bladder cancer, head and neck cancer, and a wide range of other malignancies (10, 14). However, due to its very low aqueous solubility, conventional paclitaxel like Taxol uses a Cremophor EL/ethanol vehicle as the solvent. The Cremophor EL–containing paclitaxel formulation can cause severe allergic, hypersensitivity, and anaphylactic reactions in animals and humans, which limited its application in patients with pediatric cancer (15–17). Although paclitaxel were reactive to several neuroblastoma cell lines *in vitro*, it displayed little efficacy *in vivo* in nude mice (18). In a phase I trial in children with refractory solid tumors, severe acute neurologic and allergic toxicity was encountered with 3-hour paclitaxel infusion after premedication (dexamethasone, dexchlorpheniramine) with one treatment-related death occurred (19). For reasons that are still unclear, taxanes showed minimal activity in treating solid tumors in children in several clinical trials (20–22).

Nab-paclitaxel (also known as ABI-007, Abraxane, Celgene Corporation) is a novel, solvent-free, 130 nm, protein-stabilized formulation of paclitaxel that was developed to reduce the toxicity of solvent-based paclitaxel (known as Taxol; refs. 23, 24). In human adult tumor models, nab-paclitaxel is effective in inducing regression of implanted human malignant carcinomas and prolonging survival in tumor-bearing mice (25). Clinically, nab-paclitaxel is approved globally for the treatment of metastatic breast cancer (MBC) and is also recently approved in the United States for the first-line treatment of locally advanced or metastatic NSCLC, in combination with carboplatin, in patients who are not candidates for curative surgery or radiotherapy. As limited pediatric data are currently available, in this study, we tested the antitumor activity of nab-paclitaxel against different pediatric solid tumor models to support the development of early-phase clinical trials in pediatric patients.

Materials and Methods

Materials and reagents

Nab-paclitaxel (Celgene Corporation) was supplied as a lyophilized powder and stored at room temperature until reconstitution. Nab-paclitaxel was reconstituted following the package insert with 20 mL 0.9% saline to 5 mg/mL stock solution. The dosing solutions were prepared by diluting the stock solution with 0.9% saline to the desired concentration. Paclitaxel was dissolved in dimethyl sulfoxide (DMSO; Sigma-Aldrich) to 25 mg/mL stock solution. The dosing solutions were prepared by diluting the stock solution with 0.9% saline to the desired concentration.

The Annexin V–FITC Early Apoptosis Detection Kit was purchased from Cell Signaling Technology, Inc. The cleaved caspase-3 (Asp175) antibody was obtained from Cell Signaling Technology, Inc. The anti-histone H3 (phospho S10) antibody was purchased from Abcam, Inc.

Cell culture

RH4, RH30, and RD rhabdomyosarcoma cells and KHOS osteosarcoma cells were gifts from Dr. David Malkin (The Hospital for Sick Children, Toronto, Canada). LAN-5, SK-N-BE(2), BE(2)C, and SH-SY5Y neuroblastoma cells were kindly provided by Dr. Herman Yeger (The Hospital for Sick Children). CHLA-15, CHLA-20, and CHLA-90 were obtained from the Children's Oncology Group Cell Culture and Xenograft Repository under a signed and approved Material Transfer Agreement. RH4, RH30, and RD rhabdomyosarcoma cells were cultured in Dulbecco's modified Eagle medium supplemented with 10% FBS. CHLA-15, CHLA-20, and CHLA-90 neuroblastoma cells were cultured in Iscove's modified Dulbecco's medium supplemented with 3 mmol/L L-glutamine, insulin, and transferin 5 μg/mL each and 5 ng/mL selenous acid (ITS Culture Supplement; Collaborative Biomedical Products) and 20% FBS (complete medium). LAN-5, SK-N-BE(2), BE(2)C, and SH-SY5Y neuroblastoma cells were cultured in α-minimum essential medium with 10% FBS. KHOS osteosarcoma cells were cultured in Eagle's minimum essential medium supplemented with 10% FBS.

Test animals

Female NOD/SCID (nonobese diabetic/severe combined immunodeficient) mice 4- to 6-week old were obtained from Charles River Laboratories. Animals were housed in the animal facility of the Hospital for Sick Children. These studies were conducted under the Hospital for Sick Children Animal Care Committee approval.

Published OnlineFirst August 29, 2013; DOI: 10.1158/1078-0432.CCR-13-1485

Cell viability assay

Cells were seeded into 24-well tissue culture plates at a density of 200,000 cells per well in culture medium and incubated for 24 hours at 37°C before starting drug treatment. Cells were exposed to increasing concentrations of nab-paclitaxel for 72 hours. The viability of proliferating cells in the control and treated media were measured with the Alamar Blue Assay according to manufacturer's protocol (Trek Diagnostics Systems, Inc.). Briefly, Alamar Blue was diluted 1 to 10 in the cell culture media and the fluorescent color change was monitored after 3 hours. Colorimetrical evaluation of cell proliferation was conducted using a SpectraMax Gemini spectrophotometer with 540 nm as excitation wavelength and 590 nm as emission wavelength and values expressed as relative fluorescence units. Cell viability was measured in triplicate and calculated relative to control nontreated cells.

Immunofluorescence analysis of apoptosis

Annexin V was used to detect apoptosis with the Annexin V–FITC Early Apoptosis Detection Kit (Cell Signaling Technology, Inc.). Cells were cultured (2×10^5 cells) on coverslips overnight before the treatment with nab-paclitaxel for 48 hours. For apoptosis staining with annexin V–fluorescein isothiocyanate (FITC), after incubated with annexin V–FITC according to manufacturer's protocol, the cells were washed and fixed in 2% formaldehyde before visualization under a fluorescence microscope using a dual filter set for FITC–Annexin V (green) and DAPI (nuclei staining, blue).

Xenograft development

The antitumor activity of nab-paclitaxel/paclitaxel was investigated *in vivo* against subcutaneous rhabdomyosarcoma (RH4 and RH30) and neuroblastoma [SK-N-BE(2) and CHLA-20] using NOD/SCID tumor xenografts. Briefly, tumor cells were washed three times with Hank's Balanced Salt Solution (HBSS) before injection. Mice were given a subcutaneous injection of 1×10^6 tumor cells. Tumor growth was measured weekly in two dimensions using a digital caliper and tumor volume was calculated as width$^2 \times$ length $\times$ 0.5. Once the tumor diameter reached 0.5 cm, mice were randomized into treatment groups with 7 to ten animals in each group. Nab-paclitaxel was administered either at low-dose metronomic (LDM) administration (three different doses of 2, 5, or 10 mg/kg i.v. daily) consecutively for over 3 weeks or cytotoxic dose (50 mg/kg i.v. weekly) until tumor volume reached approximately 1.5 cm^3. Paclitaxel was administered intravenously at 20 or 30 mg/kg weekly. Control mice received saline.

Tumor volume, mouse body weight, and signs of animal distress were evaluated twice or three times a week for any potential drug toxicity. Animals were sacrificed once the tumor size reached 1.5 cm^3.

In tumor rechallenge experiments, when RH4-relapsed tumors from paclitaxel treatment reached 0.5 cm in diameter, we randomized these animals into two treatment groups ($n = 3$): nab-paclitaxel and paclitaxel. For nab-paclitaxel–relapsed tumors, we randomized animals into two groups ($n = 3$): nab-paclitaxel treatment and saline control. Drugs were given with the same schedule and dosage as above. Tumor growth and animal body weight were monitored.

The anti-metastatic activity of nab-paclitaxel was further investigated in SK-N-BE(2) neuroblastoma metastatic models. Tumor cells were injected intravenously into the lateral tail vein (26-gauge needle, 1×10^6 cells in 100 μL total volume). Mice were randomized into two groups (control and nab-paclitaxel 50 mg/kg i.v. weekly) with 10 mice in each group and treatments started 14 days after inoculation until the event of endpoint. The event of endpoint was defined according to our animal committee guidelines as mice in severe clinical condition, such as loss of 20% of body weight, body temperature lower than 32°C, or signs of stress. The survival time of control and nab-paclitaxel treatment groups was compared and statistically analyzed.

Immunohistochemistry staining

To assess the effect of nab-paclitaxel on inducing cell-cycle arrest and apoptosis *in vivo*, SK-N-BE(2) subcutaneous xenografts treated with nab-paclitaxel or DMSO-paclitaxel were harvested at the end of study and analyzed by immunohistochemistry (IHC) for the apoptotic marker (cleaved caspase-3) and mitotic marker (phospho-histone H3). RH4 xenografts were harvested and analyzed by IHC for phospho-histone H3. Briefly, formalin-fixed, paraffin-embedded tissues were cut into 5 μm-thick sections and immunostained with the polyclonal antibodies against cleaved caspase-3 (1:50; Cell Signaling Technology, #9661) and histone H3 phospho S10 (1:2,000: Abcam, #ab5716). Heat-induced epitope retrieval was conducted and the ImmPRESS Anti-Rabbit Ig Peroxidase Reagent Kit (Vector Laboratories, #MP-7401) was used for detection followed by DAB and hematoxylin staining.

LC/MS plasma/intratumor concentration

Plasma and intratumor drug concentration was studied after single or repeated drug administration. In RH4 xenograft model, blood/tumor samples were collected 24 hours after the first dosage of nab-paclitaxel (50 mg/kg) or paclitaxel (30 mg/kg). In the SK-N-BE(2) xenograft model, paclitaxel (20 mg/kg), and nab-paclitaxel (50 mg/kg) were administered on day 1, 8 and 15. LDM nab-paclitaxel (10 mg/kg) was administered daily from day 1 to day 15. Twenty-four hours after the last dosage of nab-paclitaxel/paclitaxel, blood and tumor samples were collected and analyzed for paclitaxel concentration by liquid chromatography/tandem mass spectrometry (LC/MS–MS). The system consisted of HPLC (Agilent 1200), reverse phase column (Phenomenex Kinetex XB-C18, 2.6 u, 100A, 50 $\times$ 3.0 mm), and mass spectrometer (Sciex 4000). The analytes were eluted by gradient flow. The mobile phase A was 0.1% formic acid in water and mobile phase B was 0.1% formic acid in acetonitrile. The mobile phase ratio was 65% A and 35% B till 2.5 minutes, gradual increase to 100% B till 3.5 minutes, 100% B till 5.5 minutes and finally return to initial condition i.e., 65% A and 35% till

Published OnlineFirst August 29, 2013; DOI: 10.1158/1078-0432.CCR-13-1485

10 minutes. The run time was 10 minutes and the flow rate was 300 μL/min. Samples were ionized by electrospray ionization in positive polarity mode and acquisition was done by multiple reaction monitoring. Following mass transitions were monitored: paclitaxel (M + H): 854.5→286.1 *m/z*; docetaxel (M + H): 808.5→527.2 *m/z*. Ratio of intratumoral versus plasma concentration was calculated and compared between nab-paclitaxel and DMSO-based paclitaxel treatment groups.

Statistical analysis

Data from different experiments were presented as mean ± SD. For statistical analysis, Student *t* test for independent means was used. A P value of < 0.05 was considered significant. To compare the effects of different treatments on tumor growth *in vivo*, one-way ANOVA with Dunnett multiple comparison test was used. Mann–Whitney *U* test was used in tumor rechallenge experiments for the statistical evaluation of significant differences in growth patterns between two study groups. Survival curve comparisons were conducted using GraphPad Prism software for Kaplan–Meier survival analysis.

Results

In vitro cytotoxicity of nab-paclitaxel against pediatric tumor cell lines

To determine the efficacy of nab-paclitaxel against a wide panel of pediatric cancer cells lines, three rhabdomyosarcoma (RH4, RH30, and RD), seven neuroblastoma cell lines [CHLA-20, CHLA-15, CHLA-90, LAN-5, SK-N-BE(2), BE(2)C, and SH-SY5Y] and one osteosarcoma cell line (KHOS), were tested for viability with Alamar Blue assays after exposing cells to increasing concentrations of nab-paclitaxel *in vitro* for 72 hours. As shown in Fig. 1A, the cell viability of three rhabdomyosarcoma cell lines were reduced following increasing dose of nab-paclitaxel treatment. IC_{50} values were calculated and ranged from 0.56 to 4.68 nmol/L.

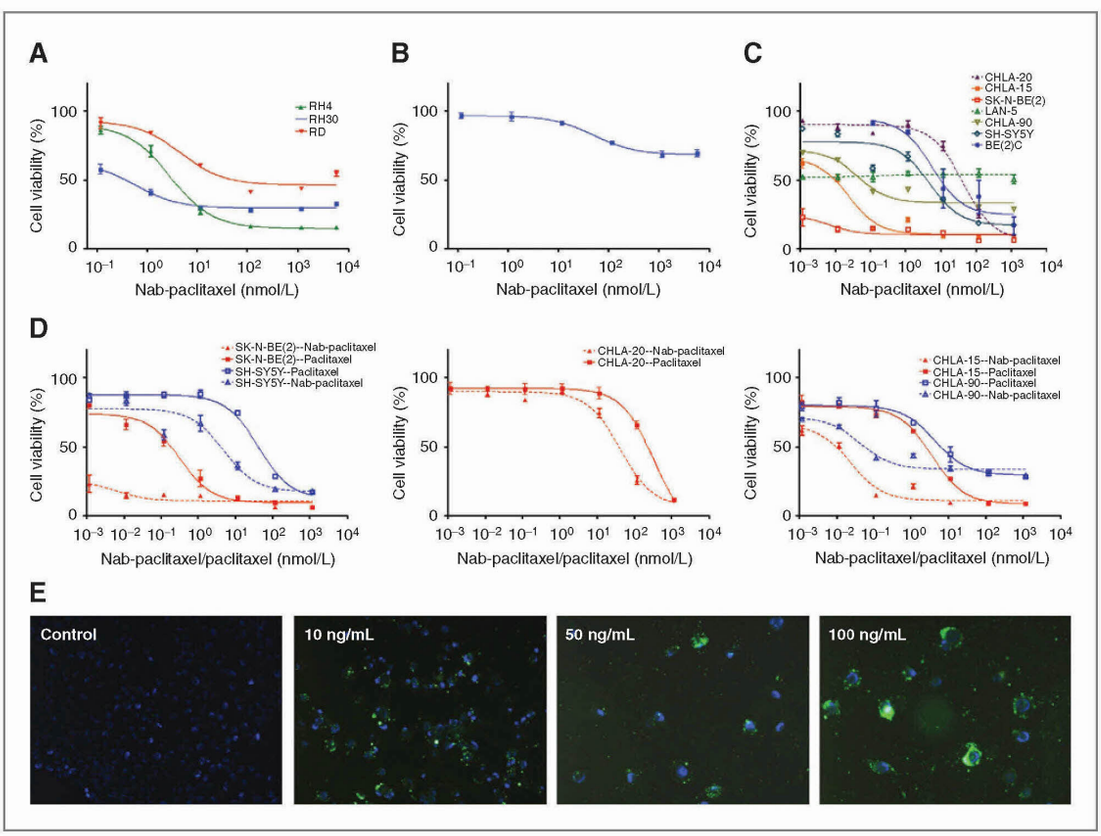

Figure 1. Effects of nab-paclitaxel on pediatric tumor cell lines *in vitro*. Alamar Blue assays were conducted after exposing tumor cells to increasing concentrations of nab-paclitaxel *in vitro* for 72 hours. Cell viability was plotted with GraphPad Prism software on three rhabdomyosarcoma cell lines, RH4, RH30, and RD (A), the osteosarcoma cell line, KHOS (B), and seven neuroblastoma cell lines, CHLA-20, CHLA-15, CHLA-90, LAN-5, SK-N-BE(2), BE(2)C, and SH-SY5Y (C). D, neuroblastoma cell lines were treated with the same concentration of paclitaxel *in vitro*. Cell viability was compared between paclitaxel and nab-paclitaxel. E, cell apoptosis was analyzed by annexin V–FITC fluorescence staining. RH4 cells were treated with 12, 60, or 120 nmol/L nab-paclitaxel *in vitro* for 48 hours followed by annexin V–FITC staining. Untreated cells are shown for comparison (control).

Published OnlineFirst August 29, 2013; DOI: 10.1158/1078-0432.CCR-13-1485

Limited response was observed with osteosarcoma cell line KHOS (Fig. 1B).

For the seven neuroblastoma cell lines, nab-paclitaxel exhibited dose-dependent cytotoxicity *in vitro*, as measured by cell viability (Fig. 1C). Different cell lines displayed variable sensitivity for nab-paclitaxel. Among all these cell lines, CHLA-20 has the highest IC_{50} (36 nmol/L), whereas LAN-5 and SK-N-BE(2) have the lowest EC_{50}. Furthermore, when neuroblastoma cell lines were treated for 72 hours *in vitro*, all the tested cell lines showed more sensitivity to nab-paclitaxel than to paclitaxel dissolved in the solvent DMSO (Fig. 1D), suggesting that paclitaxel in albumin-bound formulation in solution more readily available for tumor cell uptake.

Nab-paclitaxel–induced apoptosis in rhabdomyosarcoma cells

We further assessed cell apoptosis after *in vitro* drug treatment. Rhabdomyosarcoma RH4 cells were incubated with increasing concentrations of nab-paclitaxel for 48 hours and analyzed for apoptosis with annexin V–FITC. Annexin V–FITC–conjugated protein binds to cell surfaces expressing phosphatidylserine, an early apoptosis marker. Increased apoptotic RH4 cells as shown by annexin V–FITC–positive staining was observed following nab-paclitaxel treatment (Fig. 1E). With the higher concentration of nab-paclitaxel (60 or 120 nmol/L), most cells detached from the coveslips, but almost all the remaining cells showed annexin V–FITC–positive staining.

In vivo antitumor activity of nab-paclitaxel against rhabdomyosarcoma

The *in vivo* antitumor activity of nab-paclitaxel was evaluated in multiple pediatric tumor xenografts. In rhabdomyosarcoma models, mice bearing RH4 and RD xenografts were treated intravenously with nab-paclitaxel (50 mg/kg) and paclitaxel (30 mg/kg). The 50 mg/kg weekly dose of nab-paclitaxel is estimated to be comparable with human maximum tolerated dose (MTD; 150 mg/m^2 weekly) based on the calculation from U.S. Food and Drug Administration dose conversion guidelines. The 30 mg/kg dose of paclitaxel is the MTD in mice (26) and it is comparable with the highest dosage in adult patients too.

Both nab-paclitaxel and DMSO-paclitaxel treatments significantly inhibited RH4 tumor growth, with tumor regression observed after the second dosage on day 8 (Fig. 2A). However, animals treated with paclitaxel showed lower body weight compared with nab-paclitaxel and control animals (Fig. 2B), and 1 of 7 mice in paclitaxel group died on day 10. Especially during the first week after paclitaxel administration, all mice showed signs of inappetence, hunched posture, dry feces, and significant body weight loss. Necropsy of the dead animal showed that both cecum and colon were distended with hard stools. Our results showed that paclitaxel, even at a lower dose, had higher toxicity compared with nab-paclitaxel. In the RH4 model, increased local relapse-free intervals were observed with nab-paclitaxel treatment (37.7 $\pm$ 3.2 days) comparing to paclitaxel (13.6 $\pm$ 2.07 days).

In RD xenograft model, both paclitaxel and nab-paclitaxel treatment significantly inhibited tumor growth, but tumor shrinkage was only observed in nab-paclitaxel–treated tumors (Fig. 2C).

Efficacy of nab-paclitaxel in paclitaxel-resistant or -relapsed rhabdomyosarcoma xenografts

In RH4 xenografts, either paclitaxel or nab-paclitaxel was administered on day 1, 8, and 15. Complete regression was observed in paclitaxel-treated mice after day 31 (Fig. 2D). However, all paclitaxel-treated animals showed tumor relapse after 11 to 15 days. On day 52, when paclitaxel-relapsed tumors reached 0.5 cm in diameter, we randomized animals into two treatment groups: nab-paclitaxel and paclitaxel. Drugs were given on day 52, 59, and 66 with the same schedule and dosage as above. As shown in Fig. 2D, relapse RH4 xenografts were drug resistant against paclitaxel, but remained sensitive to nab-paclitaxel treatment. Tumor regression was observed in all relapsed tumors, which were treated again with nab-paclitaxel ($P < 0.05$; Mann–Whitney *U* test).

Complete regression was observed in nab-paclitaxel–treated mice after day 29 (Fig. 2E). Six of 7 animals developed relapsed tumor after 37 to 42 days. On day 75, when nab-paclitaxel–relapsed tumors reached 0.5 cm in diameter, we randomized animals into two groups: nab-paclitaxel treatment and saline control. Nab-paclitaxel or saline was given on day 75, 82, and 87 with the same schedule and dosage as above. As seen in Fig. 2E, when we treated those relapsed RH4 tumors with nab-paclitaxel (50 mg/kg, weekly) again, refractory tumors remained responsive to nab-paclitaxel. We observed significant difference between nab-paclitaxel rechallenge and control tumor volumes ($P < 0.05$; Mann–Whitney *U* test).

In RD xenograft model, paclitaxel (30 mg/kg, weekly) or nab-paclitaxel (50 mg/kg, weekly) was administered on day 1 and 8. Tumor regression was observed with nab-paclitaxel treatment. Comparing with control animals, paclitaxel treatment was able to slow the growth of RD tumors, but those tumors grew progressively with no signs of tumor regression. On day 15, when we replaced the paclitaxel drug treatment with nab-paclitaxel (50 mg/kg, weekly), those tumors regressed rapidly after the first dosage of nab-paclitaxel (Fig. 2C).

Antitumor effects of nab-paclitaxel with different regimens in neuroblastoma models

We further compared different schedules and doses of nab-paclitaxel, LDM, and standard MTD schedule in neuroblastoma xenograft models. Subcutaneous mouse xenograft tumors [SK-N-BE(2) and CHLA-20] were treated with either vehicle alone, nab-paclitaxel at 2, 5, and 10 mg/kg daily or 50 mg/kg weekly. Control mice received saline. Increasing doses of nab-paclitaxel at 2, 5, 10 mg/kg i.v., daily clearly showed greater tumor growth inhibition with SK-N-BE(2) in a dose-dependent manner (Fig. 3A). The 2 mg/kg/d

Published OnlineFirst August 29, 2013; DOI: 10.1158/1078-0432.CCR-13-1485

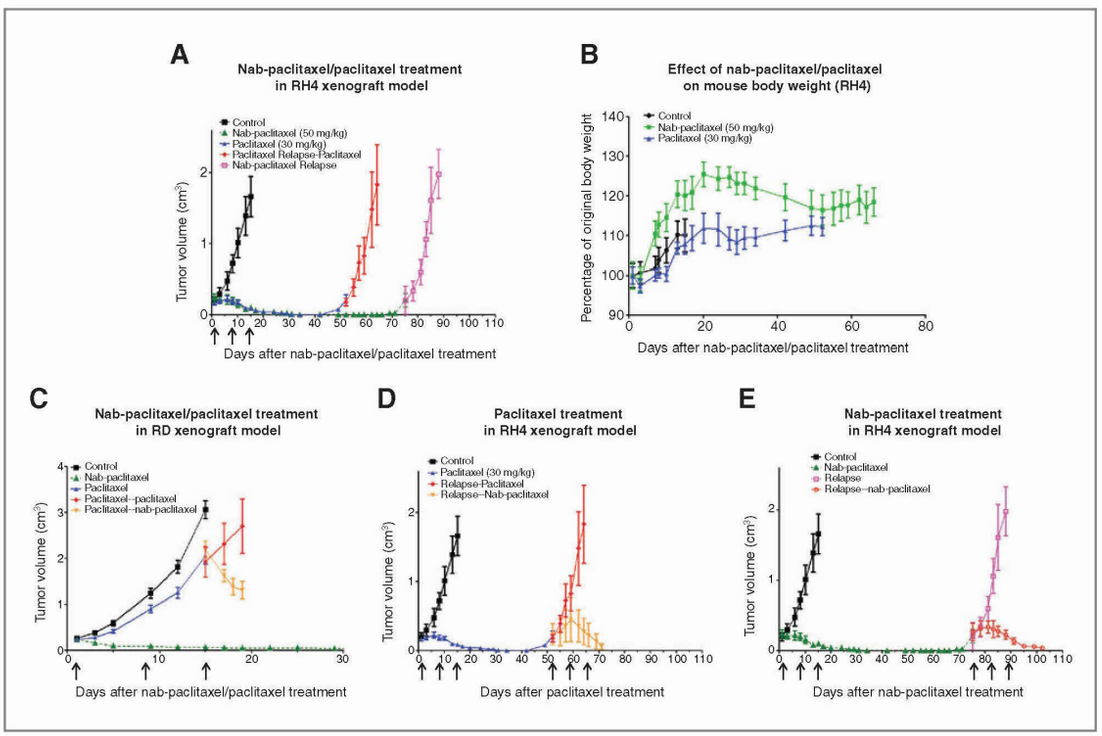

Figure 2. Effects of nab-paclitaxel on the growth of rhabdomyosarcoma xenografts. Small arrows indicate time points of drug administration. A, in RH4 xenografts, when xenograft tumors reached above 0.5 cm in diameter, mice were randomized into 3 groups (control, nab-paclitaxel treatment, and paclitaxel treatment) with 7 animals in each group. Paclitaxel or nab-paclitaxel was administered on day 1, 8, and 15 at the dose of 30 and 50 mg/kg, respectively. Tumor volume was measured and calculated as width^2 × length × 0.5. Complete regression was observed in both paclitaxel and nab-paclitaxel–treated RH4 tumors. B, animal body weight was measured in RH4 model to monitor the potential drug toxicity. C, tumor growth was assessed in RD xenograft model with paclitaxel/nab-paclitaxel treatment. In the nab-paclitaxel treatment group ($n = 10$), tumor-bearing mice received nab-paclitaxel (50 mg/kg, weekly) treatment. In the paclitaxel treatment group ($n = 10$), as tumor sizes reached the endpoint after 2-week paclitaxel treatment in the paclitaxel group, we randomized those mice into two groups with 5 animals in each group on day 15: one group of animals continued receiving 30 mg/kg of paclitaxel (tumor growth curve shown in red) and the other group received 50 mg/kg of nab-paclitaxel instead (shown in orange curve). D, on day 52, when relapsed tumors from paclitaxel treatment reached 0.5 cm in diameter, we randomized these animals into two treatment groups: nab-paclitaxel and paclitaxel. Drugs were given on day 52, 59, and 66 with the same schedule and dosage as above. Tumor growth was monitored in this paclitaxel-relapsed tumor model. E, in the nab-paclitaxel-relapsed tumor model, on day 75, when relapsed tumors from nab-paclitaxel treatment reached 0.5 cm in diameter, we randomized animals into two groups: nab-paclitaxel treatment and saline control. Drugs were given on day 75, 82, and 87 with the same schedule and dosage as above.

dosage showed no significant effect on tumor growth, whereas the 5 and 10 mg/kg daily doses significantly inhibited tumor growth ($P < 0.05$, one-way ANOVA). The strongest antitumor activity was observed with nab-paclitaxel at 50 mg/kg i.v., weekly. In CHLA-20 xenograft model, nab-paclitaxel at 50 mg/kg i.v., weekly showed similar antitumor activity compared with LDM therapy at 10 mg/kg daily (Fig. 3B).

The animal survival from nab-paclitaxel treatment was further investigated in SK-N-BE(2) metastatic models. Tumor-bearing mice were treated with control vehicle or nab-paclitaxel (50 mg/kg i.v. weekly) with all treatments starting 14 days after tumor cell inoculation. As shown in Fig. 3C, nab-paclitaxel treatment significantly prolonged animal survival compared with the control group (median survival of 59 days for nab-paclitaxel group vs. 32 days for control group; $P < 0.01$). Nab-paclitaxel treatment significantly increased body weight in these mice (Fig. 3D) compared with control.

Plasma and tumor paclitaxel concentrations following nab-paclitaxel treatment

Plasma and intratumor drug concentration was measured after single or repeated drug administration (details in "Materials and Methods" section). Twenty-four hours after the last dose, blood and tumor samples were collected and analyzed for paclitaxel concentration by LC/MS. In both tumor models, nab-paclitaxel treatment displayed lower plasma paclitaxel concentrations compared with DMSO-paclitaxel, whereas the intratumor paclitaxel concentrations were higher with nab-paclitaxel groups (Fig. 4A and B). As a consequence, nab-paclitaxel had a higher tumor/plasma

Published OnlineFirst August 29, 2013; DOI: 10.1158/1078-0432.CCR-13-1485

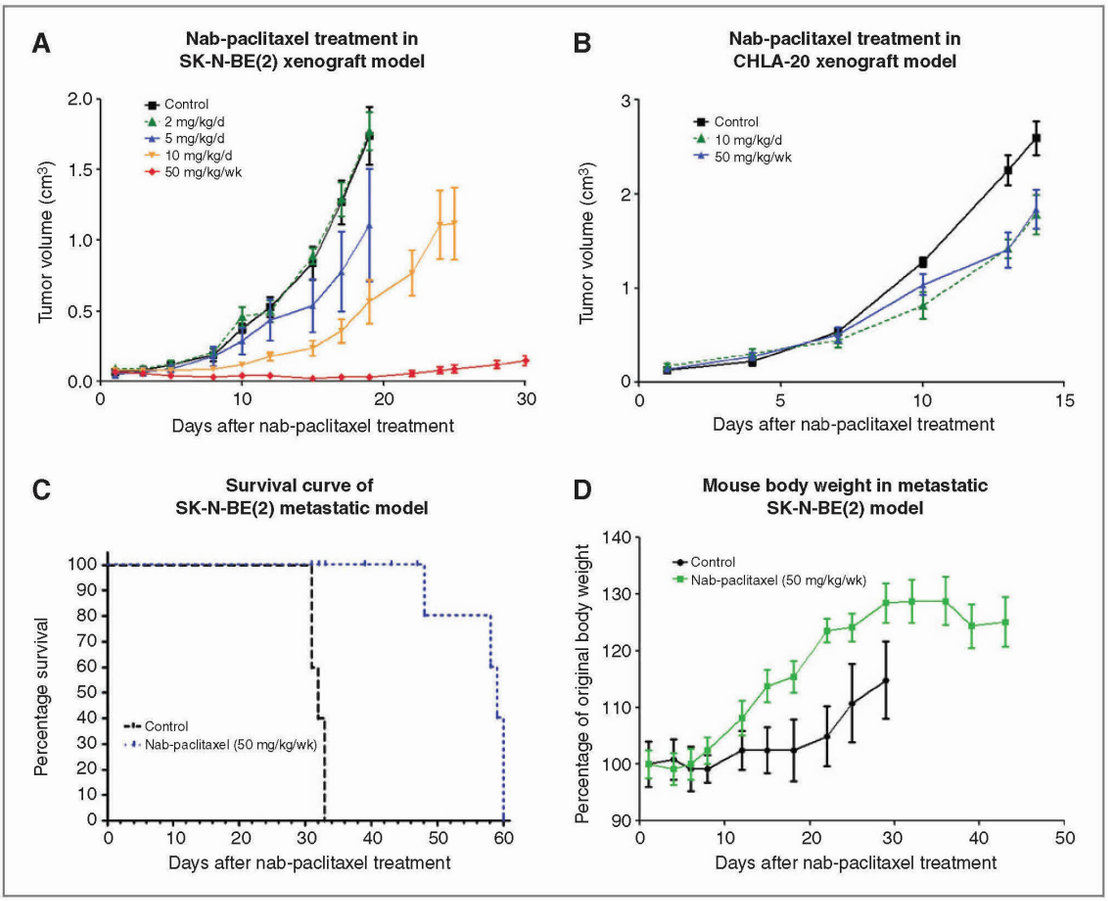

Figure 3. Antitumor effects of nab-paclitaxel with different regimens in neuroblastoma models. A, subcutaneous mouse xenograft tumors [SK-N-BE(2)] were established and animals were randomized into five groups. Each treatment group ($n = 7$) received either standard MTD of nab-paclitaxel (50 mg/kg, weekly) or LDM nab-paclitaxel (2, 5, or 10 mg/kg, daily). Control mice received saline. Tumor volume was plotted as shown. B, tumor growth was also evaluated in CHLA-20 xenograft model. Tumor-bearing mice with 10 animals in each group were treated with either standard MTD of nab-paclitaxel (50 mg/kg, weekly) or LDM nab-paclitaxel (10 mg/kg, daily). C, the animal survival from nab-paclitaxel treatment was further investigated in SK-N-BE(2) metastatic models. Tumor-bearing mice were treated with control vehicle or nab-paclitaxel (50 mg/kg i.v. weekly) with all treatments starting 14 days after tumor cell inoculation. Kaplan–Meier survival curves for nab-paclitaxel treatment and control animals are presented. D, animal body weight was monitored in SK-N-BE(2) metastatic models with/without nab-paclitaxel treatment.

paclitaxel ratio compared with DMSO-paclitaxel 24 hours after drug administration.

Nab-paclitaxel–induced cell apoptosis and cell-cycle arrest

To determine whether the antitumor activity of nab-paclitaxel was the result of tumor cells apoptosis and cell-cycle arrest, SK-N-BE(2) xenografts treated with different dosages of nab-paclitaxel were harvested at the end of study and analyzed by IHC for the apoptotic marker (cleaved caspase-3) and mitotic marker (phospho-histone H3). Corresponding with results of tumor growth inhibition, nab-paclitaxel treatment significantly increased apoptotic cell population in a dose-dependent manner compared with control tumors (Fig. 5A). Similarly, nab-paclitaxel treatment also increased phospho-histone H3–positive cells in a dose-dependent manner (Fig. 5B), suggesting that the suppression of tumor growth was attributed to the induction of apoptosis and cell-cycle arrest by nab-paclitaxel.

In a separate experiment, RH4 xenografts were harvested 48 hours after administering nab-paclitaxel (50 mg/kg, i.v.) or paclitaxel (30 mg/kg, i.v.), and tumor sections were stained for phospho-histone H3 by IHC. Significant increased population of phospho-histone H3–positive cells were observed after nab-paclitaxel and paclitaxel treatment (Fig. 5C). Combining with similar findings in neuroblastoma xenografts, it was concluded that nab-paclitaxel and paclitaxel treatment induced G_2–M cell-cycle arrest in tumors *in vivo*.

Published OnlineFirst August 29, 2013; DOI: 10.1158/1078-0432.CCR-13-1485

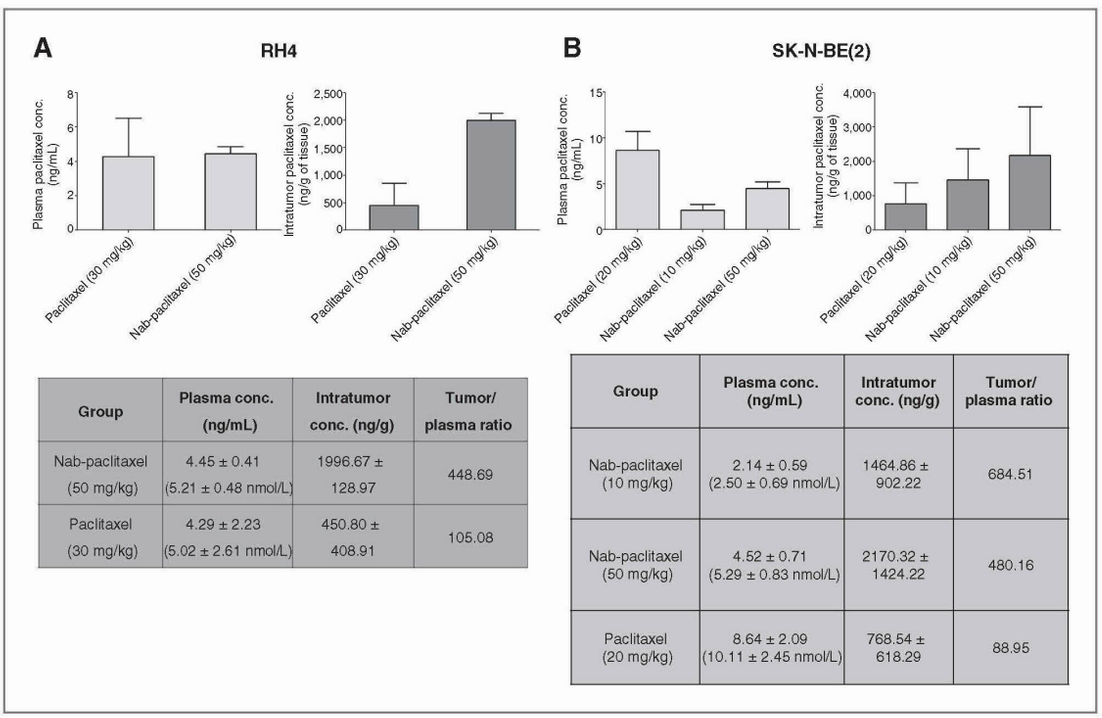

Group	Plasma conc. (ng/mL)	Intratumor conc. (ng/g)	Tumor/ plasma ratio
Nab-paclitaxel (50 mg/kg)	4.45 ± 0.41 (5.21 ± 0.48 nmol/L)	1996.67 ± 128.97	448.69
Paclitaxel (30 mg/kg)	4.29 ± 2.23 (5.02 ± 2.61 nmol/L)	450.80 ± 408.91	105.08

Group	Plasma conc. (ng/mL)	Intratumor conc. (ng/g)	Tumor/ plasma ratio
Nab-paclitaxel (10 mg/kg)	2.14 ± 0.59 (2.50 ± 0.69 nmol/L)	1464.86 ± 902.22	684.51
Nab-paclitaxel (50 mg/kg)	4.52 ± 0.71 (5.29 ± 0.83 nmol/L)	2170.32 ± 1424.22	480.16
Paclitaxel (20 mg/kg)	8.64 ± 2.09 (10.11 ± 2.45 nmol/L)	768.54 ± 618.29	88.95

Figure 4. Plasma and intratumor paclitaxel concentrations following nab-paclitaxel treatment. Mice bearing human rhabdomyosarcoma (RH4) and neuroblastoma [SK-N-BE(2)] xenografts were intravenously administered different dosages of paclitaxel (20 mg/kg weekly or 30 mg/kg weekly) or nab-paclitaxel (10 mg/kg/d for 5 consecutive days or 50 mg/kg weekly). Twenty-four hours after the last dose, blood and tumor samples were collected and analyzed for paclitaxel concentration by LC/MS. Plasma and intratumor concentrations were plotted in graphs for both RH4 (A) and SK-N-BE(2; B) models. Ratio of intratumoral and plasma concentration was calculated and compared between nab-paclitaxel and DMSO-based paclitaxel treatment groups.

Discussion

Paclitaxel has been approved worldwide for the treatment of adult solid tumors, including breast, ovarian, lung, prostate, esophageal, gastric cancer, etc. (27) Conventional formulation of paclitaxel is inconvenient and associated with significant and poorly predictable side effects largely due to the pharmaceutical vehicle Cremophor EL. In this study, we assessed a novel formulation of paclitaxel prepared by high-pressure homogenization of paclitaxel in the presence of human serum albumin, which results in a nanoparticle colloidal suspension.

Clinical studies showed that nab-paclitaxel has several advantages over solvent-based paclitaxel. These included ability to dose at higher levels of paclitaxel (MTD of 300 mg/m^2 for nab-paclitaxel every 3 weeks versus 175 mg/m^2 for conventional paclitaxel); elimination or diminution of premedication requirements for solvent-related hypersensitivity reaction; shorter infusion durations; and elimination of the need for specialized IV infusion apparatus to accommodate corrosive effects of solvent (23, 28).

Furthermore, a recent phase III trial in patients with MBC compared nab-paclitaxel with paclitaxel. Nab-paclitaxel resulted in significantly higher response rates and time to tumor progression than paclitaxel. There was no incidence of grade 3/4 hypersensitivity reactions in the group of patients treated with nab-paclitaxel, despite the absence of premedication. Toxicity data showed that nab-paclitaxel resulted in less grade four neutropenia than paclitaxel, and although the incidence of grade 3, sensory neuropathy was higher with nab-paclitaxel, the time until the neuropathy decreased to grade 2 was significantly less with nab-paclitaxel compared with paclitaxel (29).

Our results have shown that nab-paclitaxel is effective against both rhabdomyosarcoma and neuroblastoma in preclinical models. We also showed that nab-paclitaxel is more active than paclitaxel in all tumor models tested. With this new formulation, we were able to administer 50 mg/kg of nab-paclitaxel to testing animals, a much higher dosage compared with paclitaxel (30 mg/kg). No mortality and significant body weight loss were observed in nab-paclitaxel–treated animals. Toxicity studies carried out by Abraxis BioScience compared the effects of single and repeated doses of nab-paclitaxel and Taxol in a number of animal species. In all cases, the MTD of nab-paclitaxel was higher than for Taxol (26). These data

Published OnlineFirst August 29, 2013; DOI: 10.1158/1078-0432.CCR-13-1485

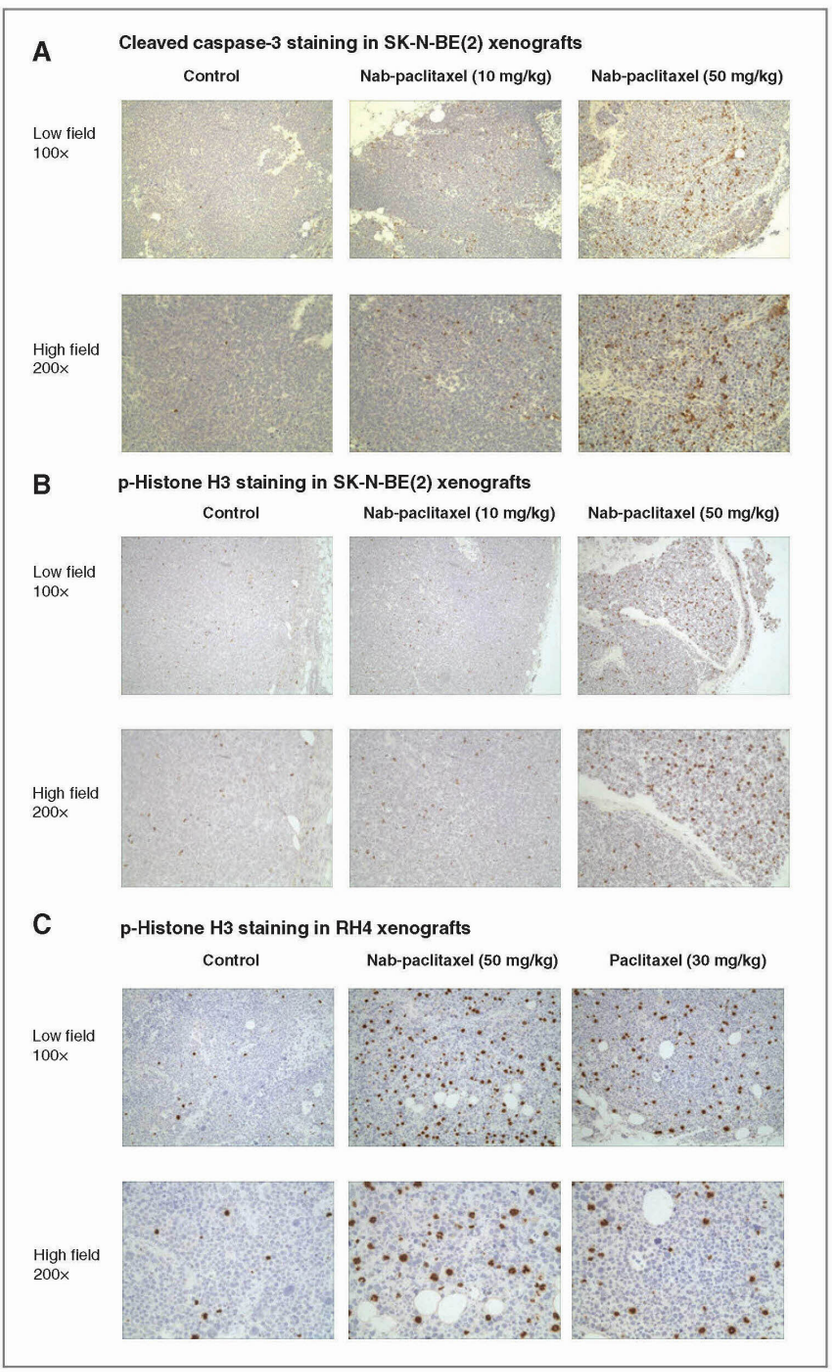

Figure 5. Nab-paclitaxel–induced cell apoptosis and cell-cycle arrest in SK-N-BE(2) and RH4 tumors. SK-N-BE(2) xenografts treated with different dosages of nab-paclitaxel were harvested at the end of study and analyzed by IHC for the cleaved caspase-3 (A) and phospho-histone H3 (B). C, in a separate experiment, RH4 xenografts were harvested 48 hours after administering nab-paclitaxel (50 mg/kg, i.v.) or paclitaxel (30 mg/kg, i.v.), and tumor sections were stained for phospho-histone H3 by IHC.

suggested that nab-paclitaxel were less toxic than Taxol and our results showed that nab-paclitaxel was better tolerated than DMSO-paclitaxel.

We also showed that, in tumor-bearing mice *in vivo*, increased intratumor and correspondingly lower plasma paclitaxel levels were observed with nab-paclitaxel compared

Published OnlineFirst August 29, 2013; DOI: 10.1158/1078-0432.CCR-13-1485

with DMSO-paclitaxel, resulting in higher tumor/plasma paclitaxel drug ratio for nab-paclitaxel. A higher intratumoral concentration produces a greater cytotoxic effect as tumor cell death is proportional to drug concentration. The lower plasma drug concentration may limit total body exposure to the cytotoxic agent resulting in reduced systemic toxicity. Nab-paclitaxel, the 130 nm nanoparticle formulation albumin-bound paclitaxel, uses the natural properties of albumin to reversibly bind paclitaxel, transport it across the endothelial cell and concentrate in tumors. The underlying mechanism is reported to involve an endothelial cell-surface albumin receptor (gp60) and an albumin-binding protein expressed by tumor cells and secreted into the tumor interstitium (secreted protein, acidic, and rich in cysteine, SPARC). gp60 is believed to mediate transcytosis of the albumin nanoparticles through endothelial cells, and binding to SPARC purportedly leads to drug accumulation in tumor tissues and thereby, enhances the therapeutic efficacy of nab-paclitaxel compared with the paclitaxel-free drug (30, 31). Additional retention of the nanoparticles in the tumor interstitium is believed to be due to the aberrant tumor angiogenesis and compromised clearance via lymphatics. This so-called "enhanced permeability and retention effect"; results in an important intratumoral drug accumulation that is even higher than that observed in plasma and normal tissues (32, 33). Clinically, nab-paclitaxel has been shown to enhance the binding of paclitaxel to albumin, microtubules, and cells and increase the tissue availability of paclitaxel when compared with solvent-based paclitaxel, as the albumin-bound paclitaxel is not trapped in the plasma compartment by Cremophor EL micelles (23, 34, 35). The results from this study were consistent with previous data in that nab-paclitaxel had lower plasma concentration (faster tissue distribution) and higer tumor accumulation compared with a solvent-based paclitaxel (25). Recent publication by Cossimo and colleagues showed that some oncogene transformed cells seem to use macropinocytosis to transport extracellular protein into the cell (36), which potentially contributes to the uptake of albumin-associated nab-paclitaxel by some tumor cells.

As with other chemotherapeutic drugs, resistance is commonly seen with paclitaxel treatment. Different mechanisms of paclitaxel resistance haven been reported including overexpression of multidrug resistance (*MDR-1*) gene (37), molecular alterations in the target molecule (β-tubulin; ref. 38), changes in apoptotic regulatory and mitosis checkpoint proteins (39), and changes in lipid composition and potentially the overexpression of interleukin-6 (40). Recent studies with array-based technology have shown that paclitaxel resistance is associated with simultaneous changes in numerous genes (41, 42). It is likely that multiple intracellular and extracellular pathways are involved in the paclitaxel-resistant phenotype. Certain types of nanoparticles were found to be able to overcome multidrug resistance mediated by the P-glycoprotein (P-gp) efflux system localized at the cancerous cell membrane. The drug export transporter P-gp can remove a large range of drugs from the cell, and upregulation of P-gp makes it possible for cancer cells to become completely resistant to some of the drugs intensively used in the clinic, notably taxanes, anthracyclines, epipodophylotoxins and *Vinca* alkaloids (43). P-gp reversion by nanoparticles was explained by a local delivery of the drug in high concentration close to the cell membrane. Such high local microconcentration of cytotoxic drugs was able to saturate P-gp (44). In this study, we observed that paclitaxel-relapsed tumors developed resistance against paclitaxel treatment, whereas those tumors are responsive to nab-paclitaxel treatment. We believe that the superior efficacy of nab-paclitaxel versus paclitaxel in the series of rechallenging experiments most possibly derived from the higher intratumor drug distribution and improved antitumor activity by nab-paclitaxel, as shown in the *in vitro* cytotoxicity study (Fig. 1) and xenograft study (Fig. 2A). As the P-gp expression in RH4 tumors remained undetectable before and after paclitaxel treatment (data not shown), it is possible that other drug export transporters, such as BCRP (ABCG2) and other MDR Proteins, are involved in paclitaxel resistance in RH4 cell lines. Interestingly, nab-paclitaxel–relapsed tumors remained sensitivity to nab-paclitaxel treatment. All tumors shrank after 1-week treatment. This finding suggests that nab-paclitaxel is less likely to trigger drug resistance compared with paclitaxel. Furthermore, studies are required to uncover the less susceptibility of nab-paclitaxel to drug resistance mechanisms.

Overall, this study showed improved antitumor activity of nab-paclitaxel against pediatric solid tumors both *in vitro* and *in vivo*. Results of this nonclinical study support further testing of nab-paclitaxel in clinical studies with pediatric solid-tumor patient population.

Disclosure of Potential Conflicts of Interest

S. Baruchel is a consultant/advisory board member of Celegne Pedaitric Scientific Advisory Board. No potential conflicts of interest were disclosed by the other authors.

Authors' Contributions

Conception and design: L. Zhang, S. Baruchel
Development of methodology: L. Zhang, S. Kumar, M. Leadley, S. Baruchel
Acquisition of data (provided animals, acquired and managed patients, provided facilities, etc.): L. Zhang, P. Marrano, M. Leadley, E. Elias, P. Thorner, S. Baruchel
Analysis and interpretation of data (e.g., statistical analysis, biostatistics, computational analysis): L. Zhang, P. Marrano, S. Kumar, M. Leadley, E. Elias, S. Baruchel
Writing, review, and/or revision of the manuscript: L. Zhang, P. Marrano, S. Kumar, S. Baruchel
Administrative, technical, or material support (i.e., reporting or organizing data, constructing databases): L. Zhang, P. Marrano, M. Leadley, S. Baruchel
Study supervision: S. Baruchel

Acknowledgments

The authors thank Drs. Shihe Hou, Daniel Pierce, Carla Heise, and Ileana Elias for their comments on our study. Mass Spectrometry analysis was conducted by Michael Leadley and Ashley St. Pierre at the Analytical Facility for Bioactive Molecules (AFBM) of the Centre for the Study of Complex Childhood Diseases (CSCCD) at the Hospital for Sick Children, Toronto, Ontario. CSCCD was supported by the Canadian Foundation for Innovation (CFI).

Published OnlineFirst August 29, 2013; DOI: 10.1158/1078-0432.CCR-13-1485

Grant Support

This work was supported by Celgene Corporation and James Birrell Neuroblastoma Research Fund.

The costs of publication of this article were defrayed in part by the payment of page charges. This article must therefore be hereby marked *advertisement* in accordance with 18 U.S.C. Section 1734 solely to indicate this fact.

Received May 30, 2013; revised August 9, 2013; accepted August 17, 2013; published OnlineFirst August 29, 2013.

References

1. Coppes MJ, Dome JS. Pediatric Clinics of North America: pediatric oncology. Preface Pediatr Clin North Am 2008;55:xv–xvi.
2. Davenport KP, Blanco FC, Sandler AD. Pediatric malignancies: neuroblastoma, Wilm's tumor, hepatoblastoma, rhabdomyosarcoma, and sacroccygeal teratoma. Surg Clin North Am 2012;92:745–67.
3. Pappo AS, Shapiro DN, Crist WM. Rhabdomyosarcoma. Biology and treatment. Pediatr Clin North Am 1997;44:953–72.
4. Huh WW, Skapek SX. Childhood rhabdomyosarcoma: new insight on biology and treatment. Curr Oncol Rep 2010;12:402–10.
5. Dantonello TM, Int-Veen C, Winkler P, Leuschner I, Schuck A, Schmidt BF, et al. Initial patient characteristics can predict pattern and risk of relapse in localized rhabdomyosarcoma. J Clin Oncol 2008;26:406–13.
6. McCarville MB, Spunt SL, Pappo AS. Rhabdomyosarcoma in pediatric patients: the good, the bad, and the unusual. AJR Am J Roentgenol 2001;176:1563–9.
7. Howman-Giles R, Shaw PJ, Uren RF, Chung DK. Neuroblastoma and other neuroendocrine tumors. Semin Nucl Med 2007;37:286–302.
8. Mugishima H. Current status of molecular biology and treatment strategy for neuroblastoma. Int J Clin Oncol 2012;17:189.
9. Ora I, Eggert A. Progress in treatment and risk stratification of neuroblastoma: impact on future clinical and basic research. Semin Cancer Biol 2011;21:217–28.
10. Horwitz SB, Lothstein L, Manfredi JJ, Mellado W, Parness J, Roy SN, et al. Taxol: mechanisms of action and resistance. Ann N Y Acad Sci 1986;466:733–44.
11. Ding AH, Porteu F, Sanchez E, Nathan CF. Shared actions of endotoxin and taxol on TNF receptors and TNF release. Science 1990;248:370–2.
12. Carboni JM, Singh C, Tepper MA. Taxol and lipopolysaccharide activation of a murine macrophage cell line and induction of similar tyrosine phosphoproteins. J Natl Cancer Inst Monogr 1993:(15)95–101. http://www.ncbi.nlm.nih.gov/pubmed/?term=Taxol+and+lipopolysaccharide+activation+of+a+murine+macrophage+cell+line+and+induction+of+similar+tyrosine+phosphoproteins.
13. Lanni JS, Lowe SW, Licitra EJ, Liu JO, Jacks T. p53-independent apoptosis induced by paclitaxel through an indirect mechanism. Proc Natl Acad Sci U S A 1997;94:9679–83.
14. Schiff PB, Fant J, Horwitz SB. Promotion of microtubule assembly *in vitro* by taxol. Nature 1979;277:665–7.
15. Rowinsky EK, Eisenhauer EA, Chaudhry V, Arbuck SG, Donehower RC. Clinical toxicities encountered with paclitaxel (Taxol). Semin Oncol 1993;20:1–15.
16. Kloover JS, den Bakker MA, Gelderblom H, van Meerbeeck JP. Fatal outcome of a hypersensitivity reaction to paclitaxel: a critical review of premedication regimens. Br J Cancer 2004;90:304–5.
17. Szebeni J, Muggia FM, Alving CR. Complement activation by Cremophor EL as a possible contributor to hypersensitivity to paclitaxel: an *in vitro* study. J Natl Cancer Inst 1998;90:300–6.
18. Vassal G, Terrier-Lacombe MJ, Bissery MC, Venuat AM, Gyergyay F, Benard J, et al. Therapeutic activity of CPT-11, a DNA-topoisomerase I inhibitor, against peripheral primitive neuroectodermal tumour and neuroblastoma xenografts. Br J Cancer 1996;74:537–45.
19. Doz F, Gentet JC, Pein F, Frappaz D, Chastagner P, Moretti S, et al. Phase I trial and pharmacological study of a 3-hour paclitaxel infusion in children with refractory solid tumours: a SFOP study. Br J Cancer 2001;84:604–10.
20. Hayashi RJ, Blaney S, Sullivan J, Weitman S, Vietti T, Bernstein ML. Phase 1 study of paclitaxel administered twice weekly to children with refractory solid tumors: a pediatric oncology group study. J Pediatr Hematol Oncol 2003;25:539–42.
21. Hurwitz CA, Strauss LC, Kepner J, Kretschmar C, Harris MB, Friedman H, et al. Paclitaxel for the treatment of progressive or recurrent childhood brain tumors: a pediatric oncology phase II study. J Pediatr Hematol Oncol 2001;23:277–81.
22. Kretschmar CS, Kletzel M, Murray K, Thorner P, Joshi V, Marcus R, et al. Response to paclitaxel, topotecan, and topotecan-cyclophosphamide in children with untreated disseminated neuroblastoma treated in an upfront phase II investigational window: a pediatric oncology group study. J Clin Oncol 2004;22:4119–26.
23. Ibrahim NK, Desai N, Legha S, Soon-Shiong P, Theriault RL, Rivera E, et al. Phase I and pharmacokinetic study of ABI-007, a Cremophor-free, protein-stabilized, nanoparticle formulation of paclitaxel. Clin Cancer Res 2002;8:1038–44.
24. Sparreboom A, Scripture CD, Trieu V, Williams PJ, De T, Yang A, et al. Comparative preclinical and clinical pharmacokinetics of a cremophor-free, nanoparticle albumin-bound paclitaxel (ABI-007), and paclitaxel formulated in Cremophor (Taxol). Clin Cancer Res 2005;11:4136–43.
25. Desai N, Trieu V, Yao Z, Louie L, Ci S, Yang A, et al. Increased antitumor activity, intratumor paclitaxel concentrations, and endothelial cell transport of cremophor-free, albumin-bound paclitaxel, ABI-007, compared with cremophor-based paclitaxel. Clin Cancer Res 2006;12:1317–24.
26. Singla AK, Garg A, Aggarwal D. Paclitaxel and its formulations. Int J Pharm 2002;235:179–92.
27. Mekhail TM, Markman M. Paclitaxel in cancer therapy. Expert Opin Pharmacother 2002;3:755–66.
28. Nyman DW, Campbell KJ, Hersh E, Long K, Richardson K, Trieu V, et al. Phase I and pharmacokinetics trial of ABI-007, a novel nanoparticle formulation of paclitaxel in patients with advanced nonhematologic malignancies. J Clin Oncol 2005;23:7785–93.
29. O'Shaughnessy J TS, Davidson N, et al. ABI-007 (ABRAXANE™), a nanoparticle albumin-bound (nab) paclitaxel demonstrates superior efficacy versus taxol in MBC: a phase III trial [abstract]. In: Proceedings from the 26th Annual San Antonio Breast Cancer Symposium; 2003; San Antonio, TX: 2003. Abstract No. 44, p. 182. San Antonio, Texas.
30. Moreno-Aspitia A, Perez EA. Nanoparticle albumin-bound paclitaxel (ABI-007): a newer taxane alternative in breast cancer. Future Oncol 2005;1:755–62.
31. Gradishar WJ. Albumin-bound paclitaxel: a next-generation taxane. Expert Opin Pharmacother 2006;7:1041–53.
32. Matsumura Y, Maeda H. A new concept for macromolecular therapeutics in cancer chemotherapy: mechanism of tumoritropic accumulation of proteins and the antitumor agent smancs. Cancer Res 1986;46:6387–92.
33. Duncan JP, Pameijer CH. Retention of parallel-sided titanium posts cemented with six luting agents: an *in vitro* study. J Prosthet Dent 1998;80:423–8.
34. Sparreboom A, van Zuylen L, Brouwer E, Loos WJ, de Bruijn P, Gelderblom H, et al. Cremophor EL-mediated alteration of paclitaxel distribution in human blood: clinical pharmacokinetic implications. Cancer Res 1999;59:1454–7.
35. ten Tije AJ, Verweij J, Loos WJ, Sparreboom A. Pharmacological effects of formulation vehicles: implications for cancer chemotherapy. Clin Pharmacokinet 2003;42:665–85.
36. Commisso C, Davidson SM, Soydaner-Azeloglu RG, Parker SJ, Kamphorst JJ, Hackett S, et al. Macropinocytosis of protein is an amino acid supply route in Ras-transformed cells. Nature 2013;497:633–7.
37. Jang SH, Wientjes MG, Au JL. Kinetics of P-glycoprotein-mediated efflux of paclitaxel. J Pharmacol Exp Ther 2001;298:1236–42.

Published OnlineFirst August 29, 2013; DOI: 10.1158/1078-0432.CCR-13-1485

38. Giannakakou P, Sackett DL, Kang YK, Zhan Z, Buters JT, Fojo T, et al. Paclitaxel-resistant human ovarian cancer cells have mutant beta-tubulins that exhibit impaired paclitaxel-driven polymerization. J Biol Chem 1997;272:17118–25.
39. Yusuf RZ, Duan Z, Lamendola DE, Penson RT, Seiden MV. Paclitaxel resistance: molecular mechanisms and pharmacologic manipulation. Curr Cancer Drug Targets 2003;3:1–19.
40. Duan Z, Lamendola DE, Penson RT, Kronish KM, Seiden MV. Over-expression of IL-6 but not IL-8 increases paclitaxel resistance of U-2OS human osteosarcoma cells. Cytokine 2002;17:234–42.
41. Duan Z, Feller AJ, Penson RT, Chabner BA, Seiden MV. Discovery of differentially expressed genes associated with paclitaxel resistance using cDNA array technology: analysis of interleukin (IL) 6, IL-8, and monocyte chemotactic protein 1 in the paclitaxel-resistant phenotype. Clin Cancer Res 1999;5:3445–53.
42. Duan Z, Lamendola DE, Duan Y, Yusuf RZ, Seiden MV. Description of paclitaxel resistance-associated genes in ovarian and breast cancer cell lines. Cancer Chemother Pharmacol 2005;55:277–85.
43. Gottesman MM. Mechanisms of cancer drug resistance. Annu Rev Med 2002;53:615–27.
44. Colin de Verdiere A, Dubernet C, Nemati F, Poupon MF, Puisieux F, Couvreur P. Uptake of doxorubicin from loaded nanoparticles in multidrug-resistant leukemic murine cells. Cancer Chemother Pharmacol 1994;33:504–8.

Published OnlineFirst August 29, 2013; DOI: 10.1158/1078-0432.CCR-13-1485

AACR American Association for Cancer Research

Clinical Cancer Research

Nab-Paclitaxel Is an Active Drug in Preclinical Model of Pediatric Solid Tumors

Libo Zhang, Paula Marrano, Sushil Kumar, et al.

Clin Cancer Res 2013;19:5972-5983. Published OnlineFirst August 29, 2013.